

# Compact Modal Interferometer Built With Tapered Microstructured Optical Fiber

Joel Villatoro, Vladimir P. Minkovich, *Member, IEEE*, and David Monzón-Hernández, *Member, IEEE*

**Abstract**—A modal interferometer was built with tapered large-mode-area microstructured optical fiber (MOF). The tapering was introduced by slowly stretching the fiber while it was heated with a high temperature flame torch. With this “slow-and-hot” tapering process, the MOF air holes collapse and the taper waist is transformed into a solid unclad multimode fiber. This allows the coupling between the fundamental  $HE_{11}$  MOF mode and the  $HE_{1m}$  modes of the solid fiber. The beating of the  $HE_{1m}$  modes makes the transmission spectra of the taper to exhibit an oscillatory pattern. The influence of the taper geometry and wavelength on the interference pattern is discussed. The interferometer can be used for diverse applications.

**Index Terms**—Microstructured optical fibers (MOFs), modal interference, optical fiber interferometers, optical fiber sensors, tapered fibers, variable attenuator.

## I. INTRODUCTION

ALL-FIBER interferometers are important devices since they are useful in diverse applications; ultrahigh-resolution metrology and light modulation are just two examples. Fiber interferometers can also be key devices in modern instruments such as gyroscopes. So far, different approaches have been proposed to construct interferometers with conventional optical fibers [1]–[6]. The most compact ones are modal interferometers since they can be constructed in a short section of optical fiber [3]–[6]. Modal interferometers exploit the relative phase displacement of the first two fiber modes  $HE_{11}$  and  $HE_{21}$  (or  $LP_{01}$  and  $LP_{11}$ ). Some drawbacks of these interferometers are, among others, the critical launching conditions, the polarization and temperature dependence, and the limited wavelength range ( $\sim 150$  nm) in which they operate.

The advent of microstructured optical fibers (MOFs) enables new possibilities to construct interferometers that can be important for many new application areas. By cascading two identical long-period gratings or by using an MOF with air holes of different diameters, novel modal interferometers can be constructed [7], [8]. An advantage of these approaches is the broad operating range ( $\sim 650$  nm) of the interferometers. However, the requisite of two identical gratings, the critical launching condi-

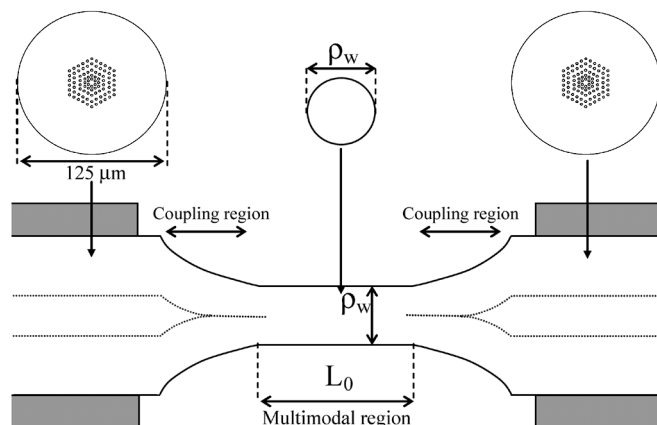


Fig. 1. Schematic representation of a modal interferometer based on tapered MOF.  $L_0$  and  $\rho_w$  are, respectively, the length and diameter of the solid waist. The shadowed area represents the polymer coating of the MOF.

tions, or the polarization and temperature dependences are still an inconvenient.

Here we demonstrate that a tapered MOF with collapsed air holes over a localized region is suitable for the construction of compact modal interferometers (see Fig. 1). By collapsing the air holes, a zone of the MOF is transformed into a solid unclad multimode optical fiber. As a consequence, the fundamental  $HE_{11}$  mode of the holey fiber is coupled to the  $HE_{1m}$  modes of the solid fiber. The beating between the modes makes the transmission of the taper versus wavelength to exhibit an oscillatory pattern. The influences of the taper diameter, length, and wavelength on the performance of the interferometer are discussed. As an application, we demonstrate an in-line variable attenuator for the wavelength of 1550 nm.

## II. DEVICE FABRICATION AND WORKING MECHANISM

A large-mode-area MOF, with solid core and four full rings of air holes in the cladding [9], was employed to construct a modal interferometer. Such a fiber had the following parameters: core diameter of  $11 \mu\text{m}$ , average hole diameter of  $2.7 \mu\text{m}$ , average hole spacing (pitch) of  $5.45 \mu\text{m}$ , and outside diameter of  $125 \mu\text{m}$ . This MOF guides light by means of the modified total internal reflection effect and it is single mode from 600 nm [9]. The fiber was tapered by gently elongating it while a zone of length  $L_0$  was heated with a high temperature oscillating flame torch. With this “slow-and-hot” tapering process, one gets a uniform-waist tapered MOF in which the air holes collapse (see Fig. 1). Our process is the opposite of the “fast-and-cold” method proposed previously for tapering MOFs, preserving the holey structure (see, for example, [10]).

Manuscript received November 29, 2005; revised March 7, 2006. This work was supported by the Consejo Nacional de Ciencia y Tecnología, Mexico, under Grant 42 986-F and Grant P46972-F, and by the “Ramón and Cajal” Program of the Ministerio de Educación y Ciencia, Spain.

J. Villatoro is with the ICFO-Institut de Ciències Fotòniques, 08860 Castelldefels, Barcelona, Spain (e-mail: joel.villatoro@icfo.es).

V. P. Minkovich and D. Monzón-Hernández are with Centro de Investigaciones en Óptica A. C., 37150 León GTO, Mexico (e-mail: vladimir@cio.mx; dmzonon@cio.mx).

Digital Object Identifier 10.1109/LPT.2006.875520

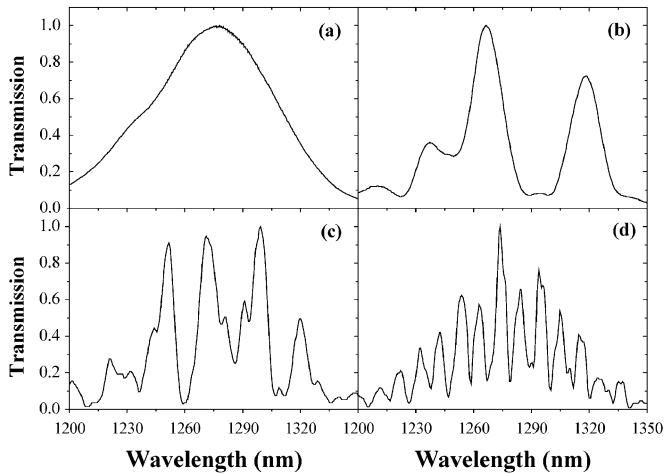


Fig. 2. Transmission spectra of an MOF (a) before and (b) after tapering to  $\rho_w = 28 \mu\text{m}$ , (c)  $\rho_w = 20 \mu\text{m}$ , and (d)  $\rho_w = 15 \mu\text{m}$ .  $L_0 = 3 \text{ mm}$  in all cases.

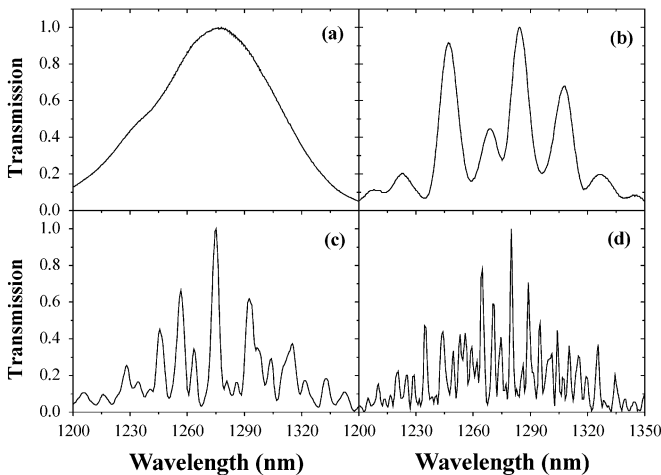


Fig. 3. Transmission spectra of an MOF (a) before and (b) after tapering to  $\rho_w = 28 \mu\text{m}$ , (c)  $\rho_w = 20 \mu\text{m}$ , and (d)  $\rho_w = 15 \mu\text{m}$ .  $L_0 = 10 \text{ mm}$  in all cases.

To monitor the fabrication of the tapers, we injected light from different light-emitting diodes (LEDs) and analyzed the output with an optical spectrum analyzer. In Figs. 2 and 3, we show the normalized transmission spectra of our large-mode-area MOF before and after the tapering. The spectra before the tapering are basically the output spectrum of the LED [see Figs. 2(a) and 3(a)]. However, after the tapering, the spectra exhibit an oscillatory pattern that depends on  $\rho_w$  or  $L_0$ . The spectra of Fig. 2(b), (c), and (d) correspond, respectively, to tapers with  $\rho_w = 28, 20,$  and  $15 \mu\text{m}$ .  $L_0 = 3 \text{ mm}$  in all three samples. The spectra shown in Fig. 3(b), (c), and (d) correspond to three other tapers, also with  $\rho_w = 28, 20,$  and  $15 \mu\text{m}$ , but in which  $L_0 = 10 \text{ mm}$ . The figures clearly show that the interference peaks become narrower for thinner (or longer) tapers. Note that the interference peaks shown in Fig. 3(b), (c), and (d) are narrower than those shown, respectively, in Fig. 2(b), (c), and (d). Tapers with waist diameters of  $28, 20,$  and  $15 \mu\text{m}$  and  $L_0 = 6 \text{ mm}$  exhibited transmission spectra that were between those shown in Figs. 2 and 3.

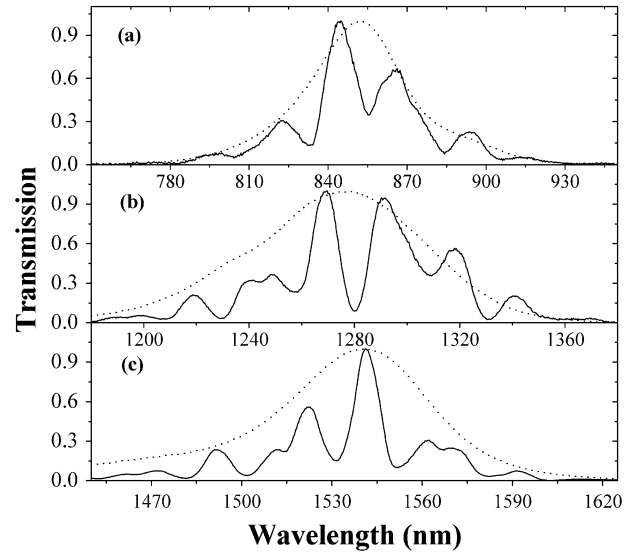


Fig. 4. Normalized transmission spectra, measured with different LEDs, of an MOF before (dotted lines) and after (continuous lines) the tapering. In all cases,  $\rho_w = 25 \mu\text{m}$  and  $L_0 = 8 \text{ mm}$ .

In Fig. 4, we show the normalized transmission spectra of a taper with  $\rho_w = 25 \mu\text{m}$  and  $L_0 = 8 \text{ mm}$ . Such spectra were obtained with three LEDs with peak emission at 850, 1280, and 1540 nm. It can be noted that the spectra of the tapers exhibit interference ripples regardless of the LED employed. This shows the broad range of wavelengths ( $\sim 900 \text{ nm}$ ) in which taper-based modal interferometers may operate. It is worth noting that the devices work with low-coherence broadband optical sources which are low cost. It should be pointed out that the losses introduced by the tapering were below to 3 dB in all the samples we fabricated, also that the spectra were normalized with respect to the highest peak.

The series of peaks shown in Figs. 2, 3, and 4 are a consequence of a coupling–beating–coupling phenomenon. Note that the solid section of the taper functions like an unclad solid multimode optical fiber which can support  $\text{HE}_{1m}$  modes. The solid section is the beating region of the interferometer. In the contracting (expanding) zone of the taper coupling between the fundamental  $\text{HE}_{11}$  mode of the holey fiber and the  $\text{HE}_{1m}$  modes of the solid fiber occurs. Thus, a tapered MOF with collapsed air holes over a localized region can be considered as a modal interferometer. The contracting and expanding zones are equivalent to couplers in a fiber-optic Mach–Zehnder interferometer, while the modes of the solid section are equivalent to the arms. The beating between the modes of the solid region makes the transmission spectrum of a tapered MOF to exhibit the interference ripples of Figs. 2, 3, and 4.

When the taper diameter decreases, or when the length of the taper increases, the separation between the propagation constants of the interfering modes increases and their beat length decreases. Therefore, the wavelength separation between the interference peaks is reduced. That is why the peaks become narrower when the taper diameter diminishes, or when  $L_0$  is increased. For sensing applications, narrow peaks are desirable since their monitoring is easier. During the tapering, one can control  $\rho_w$  and  $L_0$ , therefore, the interference peaks in this type of interferometers may be tailored. It should be pointed out that

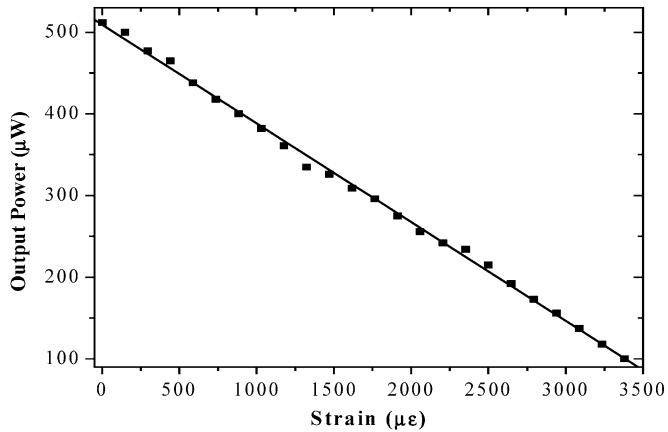


Fig. 5. Output power as a function of the applied strain of a taper with  $\rho_w = 30 \mu\text{m}$  and  $L_0 = 6 \text{ mm}$  measured at 1550 nm. The squares are experimental points and the continuous line is a linear fit to the data.

the interference pattern is not perfectly sinusoidal since not all the interfering modes have the same intensity. Filtering or the launching conditions may help to have a regular interference pattern.

### III. APPLICATIONS AND CONCLUSIONS

The modal interferometer reported here is simpler than those based on long-period gratings or two-mode MOFs [7], [8] since one has the possibility of adjusting the geometrical parameters,  $L_0$  and  $\rho_w$ , during fabrication. Moreover, the interference peaks can be monitored *in situ* and in real time during the tapering process. The launching conditions are not critical in our device. In addition, the interferometer can operate in a broad range of wavelengths. The potential applications of a modal interferometer (like other all-fiber interferometer) are diverse.

The transmission of our device depends directly on the phase difference of the interfering modes. Such a phase difference depends on the propagation constants of the modes and also on the beat length of the interferometer. The propagation constants depend on the medium surrounding the taper. The beat length can be modified by minute elongations of the tapers. Therefore, a modal interferometer can be exploited for refractive index or strain sensing [11], [12]. The development of passive devices, such as modal or wavelength filters and attenuators are also feasible.

In Fig. 5, we show the application of our modal interferometer as an in-line variable attenuator. For this application, we used a taper with  $\rho_w = 30 \mu\text{m}$  and  $L_0 = 6 \text{ mm}$ . The light source was a laser diode with wavelength of 1550 nm and 1 mW of maximum output power. As mentioned above, the insertion losses of the taper is 3 dB. Thus, the maximum detected optical power at the output of the taper was 0.5 mW. The taper was se-

cured between two mechanical mounts with which we applied longitudinal strain to it. Note that the output power decreases linearly as the applied strain increases. The maximum attenuation in this case was 80%. The device can also be used as an intensity-modulated strain sensor which is an alternative to the wavelength-encoded strain sensor reported recently [12].

In conclusion, we have reported the fabrication of a compact modal interferometer based on tapered MOFs with collapsed air holes. The collapsing of the air holes allows transforming the taper waist into a solid multimode fiber in which the modes beat or interfere. As a consequence, the transmission of the taper versus the wavelength exhibits an oscillatory pattern. The influence of the geometrical parameters of the tapers (length and diameter) and the wavelength on the interference peaks was studied. The compact, all-fiber modal interferometer reported here can be fabricated in only a few minutes. The interferometer can be used for sensing applications and also for the development of passive devices such as filters or attenuators.

### REFERENCES

- [1] D. A. Jackson and J. D. C. Jones, "Interferometers," in *Optical Fiber Sensors: Systems and Applications*, B. Culshaw and J. Dakin, Eds. Norwood, MA: Artech House, 1989, pp. 239–280.
- [2] *Handbook of Optical Fiber Sensing Technology*, J. M. López-Higuera, Ed., Wiley, New York, 2002, pp. 227–245. Interferometry and polarimetry for optical sensing, West Sussex.
- [3] B. Y. Kim, J. N. Blake, S. Y. Huang, and H. J. Shaw, "Use of highly elliptical core fibers for two-mode fiber devices," *Opt. Lett.*, vol. 12, pp. 729–731, Sep. 1987.
- [4] A. Kumar, N. K. Goel, and R. K. Varshney, "Studies on a few-mode fiber-optic strain sensor based on LP<sub>01</sub>-LP<sub>02</sub> mode interference," *J. Lightw. Technol.*, vol. 19, no. 3, pp. 358–362, Mar. 2001.
- [5] X. Daxhelet, J. Bures, and R. Maciejko, "Temperature-independent all-fiber modal interferometer," *Opt. Fiber Technol.*, vol. 1, pp. 373–376, Oct. 1995.
- [6] S. Lacroix, F. Gonthier, R. J. Black, and J. Bures, "Tapered-fiber interferometric wavelength response: The achromatic fringe," *Opt. Lett.*, vol. 13, pp. 395–397, May 1988.
- [7] J. H. Lim, H. S. Jang, K. S. Lee, J. C. Kim, and B. H. Lee, "Mach-Zehnder interferometer formed in a photonic crystal fiber based on a pair of long-period fiber gratings," *Opt. Lett.*, vol. 29, pp. 346–348, Feb. 2004.
- [8] J. Ju, W. Jin, and M. S. Demokan, "Two-mode operation in highly birefringent photonic crystal fiber," *IEEE Photon. Technol. Lett.*, vol. 16, no. 11, pp. 2471–2474, Nov. 2004.
- [9] V. P. Minkovich, A. V. Kiryanov, A. B. Sotsky, and L. I. Sotskaya, "Large-mode-area holey fibers with a few air channels in cladding: Modeling and experimental investigation of the modal properties," *J. Opt. Soc. Amer. B*, vol. 21, pp. 1161–1169, Jun. 2004.
- [10] H. C. Nguyen, B. T. Kuhlmeier, E. C. Magi, M. J. Steel, P. Domachuk, C. L. Smith, and B. J. Eggleton, "Tapered photonic crystal fibers: Properties, characterization and applications," *Appl. Phys. B*, vol. 81, pp. 377–387, Jul. 2005.
- [11] V. P. Minkovich, J. Villatoro, D. Monzón-Hernández, S. Calixto, A. B. Sotsky, and L. I. Sotskaya, "Holey fiber tapers with resonance transmission for high-resolution refractive index sensing," *Opt. Express*, vol. 13, pp. 7609–7614, Sep. 2005.
- [12] J. Villatoro, V. P. Minkovich, and D. Monzón-Hernández, "Temperature-independent strain sensor made from tapered holey optical fiber," *Opt. Lett.*, vol. 31, pp. 305–307, Feb. 2006.